

## Washington University School of Medicine Digital Commons@Becker

---

### Open Access Publications

---

2017

# Sclerostin antibody treatment enhances rotator cuff tendon-to-bone healing in an animal model

Shivam A. Shah

*Washington University School of Medicine in St. Louis*

Ioannis Kormpakis

*Washington University School of Medicine in St. Louis*

Necat Havlioglu

*John Cochran VA Medical Center*

Michael S. Ominsky

*Amgen, Inc*

Leesa M. Galatz

*Mount Sinai Health System*

*See next page for additional authors*

Follow this and additional works at: [https://digitalcommons.wustl.edu/open\\_access\\_pubs](https://digitalcommons.wustl.edu/open_access_pubs)

---

### Recommended Citation

Shah, Shivam A.; Kormpakis, Ioannis; Havlioglu, Necat; Ominsky, Michael S.; Galatz, Leesa M.; and Thomopoulos, Stavros, "Sclerostin antibody treatment enhances rotator cuff tendon-to-bone healing in an animal model." *The Journal of Bone and Joint Surgery*.99,10. 855-864. (2017).

[https://digitalcommons.wustl.edu/open\\_access\\_pubs/5922](https://digitalcommons.wustl.edu/open_access_pubs/5922)

This Open Access Publication is brought to you for free and open access by Digital Commons@Becker. It has been accepted for inclusion in Open Access Publications by an authorized administrator of Digital Commons@Becker. For more information, please contact [engeszer@wustl.edu](mailto:engeszer@wustl.edu).

---

**Authors**

Shivam A. Shah, Ioannis Kormpakis, Necat Havlioglu, Michael S. Ominsky, Leesa M. Galatz, and Stavros Thomopoulos



A commentary by Brian C. Werner, MD, is linked to the online version of this article at [jbjs.org](http://jbjs.org).

# Sclerostin Antibody Treatment Enhances Rotator Cuff Tendon-to-Bone Healing in an Animal Model

Shivam A. Shah, PhD, Ioannis Kormpakis, MD, Necat Havlioglu, MD, Michael S. Ominsky, PhD, Leesa M. Galatz, MD, and Stavros Thomopoulos, PhD

*Investigation performed at Washington University in St. Louis, St. Louis, Missouri*

**Background:** Rotator cuff tears are a common source of pain and disability, and poor healing after repair leads to high retear rates. Bone loss in the humeral head before and after repair has been associated with poor healing. The purpose of the current study was to mitigate bone loss near the repaired cuff and improve healing outcomes.

**Methods:** Sclerostin antibody (Scl-Ab) treatment, previously shown to increase bone formation and strength in the setting of osteoporosis, was used in the current study to address bone loss and enhance rotator cuff healing in an animal model. Scl-Ab was administered subcutaneously at the time of rotator cuff repair and every 2 weeks until the animals were sacrificed. The effect of Scl-Ab treatment was evaluated after 2, 4, and 8 weeks of healing, using bone morphometric analysis, biomechanical evaluation, histological analysis, and gene expression outcomes.

**Results:** Injury and repair led to a reduction in bone mineral density after 2 and 4 weeks of healing in the control and Scl-Ab treatment groups. After 8 weeks of healing, animals receiving Scl-Ab treatment had 30% greater bone mineral density than the controls. A decrease in biomechanical properties was observed in both groups after 4 weeks of healing compared with healthy tendon-to-bone attachments. After 8 weeks of healing, Scl-Ab-treated animals had improved strength (38%) and stiffness (43%) compared with control animals. Histological assessment showed that Scl-Ab promoted better integration of tendon and bone by 8 weeks of healing. Scl-Ab had significant effects on gene expression in bone, indicative of enhanced bone formation, and no effect on the expression of genes in tendon.

**Conclusions:** This study provides evidence that Scl-Ab treatment improves tendon-to-bone healing at the rotator cuff by increasing attachment-site bone mineral density, leading to improved biomechanical properties.

**Clinical Relevance:** Scl-Ab treatment may improve outcomes after rotator cuff repair.

**Peer Review:** This article was reviewed by the Editor-in-Chief and one Deputy Editor, and it underwent blinded review by two or more outside experts. The Deputy Editor reviewed each revision of the article, and it underwent a final review by the Editor-in-Chief prior to publication. Final corrections and clarifications occurred during one or more exchanges between the author(s) and copyeditors.

Rotator cuff tears do not heal spontaneously, can progress in size over time, and motivate >250,000 surgical repairs in the United States annually<sup>1</sup>. Poor tendon-to-bone healing after repair results in an alarmingly high rate of retears at the site of attachment, ranging from 20% in young healthy patients with small tears to 94% in older patients with massive tears<sup>2,3</sup>. Rotator cuff tears are associated with loss of

bone at the healing interface and a lack of regeneration of the functionally graded, mineralized fibrocartilage found in the healthy attachment<sup>4</sup>. Bone loss has been observed at healing tendon-to-bone interfaces at multiple anatomic sites<sup>5-11</sup>. The loss of mineralized tissue is likely caused by mechanical unloading during the period from tearing through surgical repair and by high osteoclast activity during the healing period after

**Disclosure:** The study was supported by National Institutes of Health (NIH) grants F31-AR066452 and NIH R01-AR057836. Sclerostin antibody was provided by Amgen, Inc. One of the authors was an employee of Amgen, Inc. at the time of the study. On the **Disclosure of Potential Conflicts of Interest** forms, which are provided with the online version of the article, one or more of the authors checked "yes" to indicate that the author had a relevant financial relationship in the biomedical arena outside the submitted work and "yes" to indicate that the author had a patent planned for the treatment that is the subject of this article (<http://links.lww.com/JBJS/D272>).

repair<sup>10,12</sup>. Chronic rotator cuff tears lead to unloading-induced osseous changes to the humeral head<sup>13</sup>. Chronic degeneration of the muscle before repair is associated with greater bone loss in the humeral head and leads to low cellular remodeling and poor extracellular matrix formation<sup>14</sup>. However, Ditsios et al. showed that mechanical unloading is not the only factor accountable for the reduction in bone mineral density (BMD) at the healing tendon-to-bone attachment<sup>15</sup>. Injury to the flexor digitorum profundus tendon in an animal model without any alteration of limb loading resulted in a sevenfold increase in osteoclast surface after 7 days, leading to a 7% decrease in BMD after 21 days.

To address the bone loss that occurs during tendon-to-bone healing, investigators in a previous study suppressed osteoclast activity using bisphosphonate treatment<sup>8,9,16</sup>. Treatment led to improved mechanical properties in the treatment group compared with the control group. However, therapy with bisphosphonates is not ideal, especially in the younger population, because of its association with reduced bone turnover and increased risk for bone fracture<sup>17-19</sup>. Another approach to increase bone mass at the site of healing is to administer a bone-anabolic agent to stimulate new bone formation. Sclerostin antibodies that block sclerostin, a negative regulator of bone formation produced largely by osteocytes, systemically increase bone formation and bone mass in animal models and osteoporotic patients<sup>20-22</sup>. In the current study, a novel application of sclerostin antibody (Scl-Ab) treatment was tested for enhancing tendon-to-bone healing. Using a well-established animal model of the rotator cuff, we tested the hypothesis that Scl-Ab treatment would prevent bone loss during tendon-to-bone healing, leading to improved outcomes.

## Materials and Methods

### Animal Model and Study Design

Eighty-seven adult male Sprague-Dawley rats (approximately 4 months old and weighing approximately 350 g) were used in this study, as approved by the Institutional Animal Care and Use Committee. Fifty-three rats received surgical

injury and repair, and 34 rats were used as uninjured controls (the normal group). Of the 53 injured-and-repaired rats, 10 (5 that received Scl-Ab [the Scl-Ab group] and 5 that had no treatment [the control (CTL) group]) were used to study 2 weeks of healing, 20 (10 in the Scl-Ab treatment group and 10 in the CTL group) were used to study 4 weeks of healing, and 23 (12 in the Scl-Ab treatment group and 11 in the CTL group) were used to study 8 weeks of healing. Of the 34 uninjured control animals, 17 were used to study the effect of Scl-Ab treatment on the healthy rotator cuff and 17 were used as healthy untreated controls. For all animals, 1 shoulder was used for bone morphometry and/or biomechanical evaluation and the contralateral shoulder was used for histological analysis or gene expression.

For rats in the injury-and-repair groups, the supraspinatus tendon was sharply severed from the humeral head and was repaired bilaterally in each animal, as previously described<sup>23</sup>. Operatively and nonoperatively treated animals either were left untreated (the CTL group) or were administered Scl-Ab (Scl-Ab VI; Amgen). The Scl-Ab was delivered via subcutaneous injections (25 mg/kg) at the onset of the study (i.e., at the time of injury and repair for the operatively treated animals and at an equivalent age for the nonoperatively treated animals) and every 2 weeks until they were killed (the Scl-Ab group). Animals in the operatively treated CTL and Scl-Ab groups were allowed cage activity and were sacrificed after 2, 4, or 8 weeks. Animals in the nonoperatively treated CTL and Scl-Ab groups were allowed cage activity and were sacrificed after 4 weeks. Postmortem supraspinatus muscle-tendon-bone samples were dissected and assessed using bone morphometry, biomechanical evaluation, histological analysis, and gene expression. As surgery was performed bilaterally and the treatment was systemic, each animal had 2 samples available for analysis. Samples were allocated to either bone morphometry followed by biomechanical evaluation or bone morphometry followed by either histological analysis or gene expression.

At the time that the animals were killed, body weight was not significantly different between treatment groups (mean [and standard deviation] across time points, 520 ± 54 g for Scl-Ab group and 510 ± 55 g for the CTL group). No repair site failure or gap was observed in the Scl-Ab and CTL groups at the time of dissection.

### Bone Morphometric Analysis

After the animals were sacrificed, the humerus with the supraspinatus tendon and muscle attached was dissected for bone morphometric analysis (17 per group of nonoperatively treated rats, 5 per group of operatively treated rats after 2 weeks of healing, and 20 to 23 per group of operatively treated rats after 4 or 8 weeks of healing). The humeral head and tendon enthesis region

TABLE I The Modified Tendon-to-Bone Maturity Score with Evaluation of 9 Individual Outcomes on a Scale of 1 to 4\*

Individual Outcomes	Score			
	1	2	3	4
Cellularity (inflammation)	Minimal	Mild	Moderate	Marked
Presence of fibrocytes (%)	>75	51-75	26-50	≤25
Proportion of cells oriented parallel (%)	>75	51-75	26-50	≤25
Proportion of fibers oriented parallel (%)	>75	51-75	26-50	≤25
Presence of matrix	Marked	Moderate	Mild	Minimal
Insertion integrity	C(+), R(+), F(+), tidemark(+)	C(+), R(+), F(+), tidemark(-)	C(+), R(+), F(-)	C(+), R(-)
Insertion continuity (%)	>75	51-75	26-50	<25
Bone resorption at enthesis (%)	≤25	26-50	51-75	>75
Epiphyseal bone modeling (%)	≤25	26-50	51-75	>75

\*Modification of the system of Ide et al.<sup>25</sup>. A healthy (uninjured) enthesis has a combined score of 9. C = continuity, R = regularity, and F = fibrocartilage.

(approximately 5 mm) were scanned using micro-computed tomography (microCT) at a resolution of 20  $\mu\text{m}$ , 45 kVp, and 177  $\mu\text{A}$  ( $\mu\text{CT}$  40; SCANCO Medical)<sup>13,24</sup>. The region of interest included trabecular bone within the humeral head near the tendon attachment (within approximately 1 mm) and proximal to the growth plate and was determined by evaluators blinded to the treatment groups. The amount of bone in the region of interest was calculated to determine bone volume fraction (BV/TV; bone volume to total volume), BMD, trabecular number (Tb.N), trabecular thickness (Tb.Th), and trabecular spacing (Tb.Sp) were also determined.

### Biomechanical Evaluation

After killing, dissection, and microCT scanning of the animals, the supraspinatus tendon-to-bone attachment was mechanically tested in uniaxial tension (17 per group for nonoperatively treated animals and 10 to 12 per group for operatively treated animals)<sup>13</sup>. The repair-site suture was released to remove its mechanical contribution, the humeri were potted in polymethylmethacrylate, and specimens were tested in a 0.9% saline solution water bath at 37°C (Instron 5866). Samples were preconditioned for 5 cycles (5% strain, 0.2%/s), allowed 300 seconds for recovery, and pulled to failure at 0.2%/s. Strain was determined from grip-to-grip displacement. Cross-sectional area near the attachment site was measured from

microCT scans by evaluators blinded to treatment group. Load-deformation curves were used to determine maximum load and stiffness. Stress-strain curves were used to determine strength (maximum stress), modulus, and resilience (area under the curve from 0% to yield strain). The mechanism of failure was determined visually. Specimens were excluded from the data analysis if the tendon slipped out of the grip or failure occurred at the growth plate of the humeral head.

### Histological Analysis

Histological analysis was performed for the CTL and Scl-Ab-treated groups following 2, 4, and 8 weeks of healing (3 animals per group). Humerus-supraspinatus constructs were fixed in 4% paraformaldehyde for 24 hours. Samples were decalcified in 14% EDTA (ethylenediaminetetraacetic acid), dehydrated in graded ethanol, and embedded in paraffin. Five-micrometer coronal sections were stained with hematoxylin and eosin, toluidine blue, or Goldner trichrome. Additional samples were fixed for 24 hours in 4% paraformaldehyde and embedded in plastic, and 5- $\mu\text{m}$ -thick coronal sections were stained with von Kossa stain. The sections were semiquantitatively analyzed by 1 blinded observer (N.H.) using a tendon-to-bone maturity score adapted from Ide et al.<sup>24,25</sup>. Insertion continuity, bone resorption, matrix quality, cell and fiber alignment, and cellularity were part of 9 factors evaluated on a scale from

**TABLE II Names of Genes, Associated Categories, and TaqMan Assay Identification Numbers\***

Gene Name	Category	TaqMan Assay ID
Tnfrsf11b (tumor necrosis factor receptor superfamily, member 11b), OPG (osteoprotegerin)	Bone, inhibits osteoclast activity	Rn00563499_m1
Sost (sclerostin)	Bone, osteoclast activity	Rn00577971_m1
Dmp1 (dentin matrix acidic phosphoprotein)	Bone, osteoclast activity	Rn01450122_m1
RankL (receptor activator of nuclear factor kappa-B ligand), Tnfrsf11 (tumor necrosis factor [ligand] superfamily, member 11)	Bone, osteoblast activity	Rn00589289_m1
Bglap (bone gamma-carboxylglutamate protein), OCN (osteocalcin)	Bone, osteoblast activity	Rn00566386_g1
Pth1r (parathyroid hormone 1 receptor)	Bone, osteoblast activity	Rn00571596_m1
Ctsk (cathepsin K)	Bone, bone resorption	Rn00580723_m1
Dkk1 (dickkopf WNT signaling pathway inhibitor 1)	Bone, Wnt signaling antagonist	Rn01501537_m1
Lrp5 (low density lipoprotein receptor-related protein 5)	Bone, Wnt signaling	Rn01451428_m1
Runx2 (runt-related transcription factor 2)	Bone, osteoprogenitor	Rn01512298_m1
Sp7 (Osterix)	Bone, osteoprogenitor	Rn02769744_s1
Scx (scleraxis)	Tendon	Rn01504576_m1
Tnmd (tenomodulin)	Tendon	Rn00574164_m1
Col1a1 (collagen, type I, alpha 1)	Tendon	Rn01463848_m1
Col1a2 (collagen, type I, alpha 2)	Tendon	Rn01526721_m1
Col3a1 (collagen, type III, alpha 1)	Tendon	Rn01437681_m1
Col2a1 (collagen, type II, alpha 1)	Fibrocartilage	Rn01637087_m1
Acan (aggrecan)	Fibrocartilage	Rn00573424_m1
Tgfb1 (transforming growth factor, beta 1)	Fibrocartilage	Rn00572010_m1
Tgfb3 (transforming growth factor, beta 3)	Fibrocartilage	Rn00565937_m1
Mmp2 (matrix metalloproteinase 2)	Fibrocartilage	Rn01538170_m1
Sox9 (SRY [sex determining region Y]-box 9)	Fibrocartilage	Rn01751069_mH
Smo (smoothed, frizzled class receptor)	Development	Rn00563043_m1
Notch1	Development	Rn01758633_m1
Rpl13a (ribosomal protein L13A)	Housekeeping	Rn00821946_g1

\*TaqMan Gene Expression Assays are manufactured by ThermoFisher Scientific.

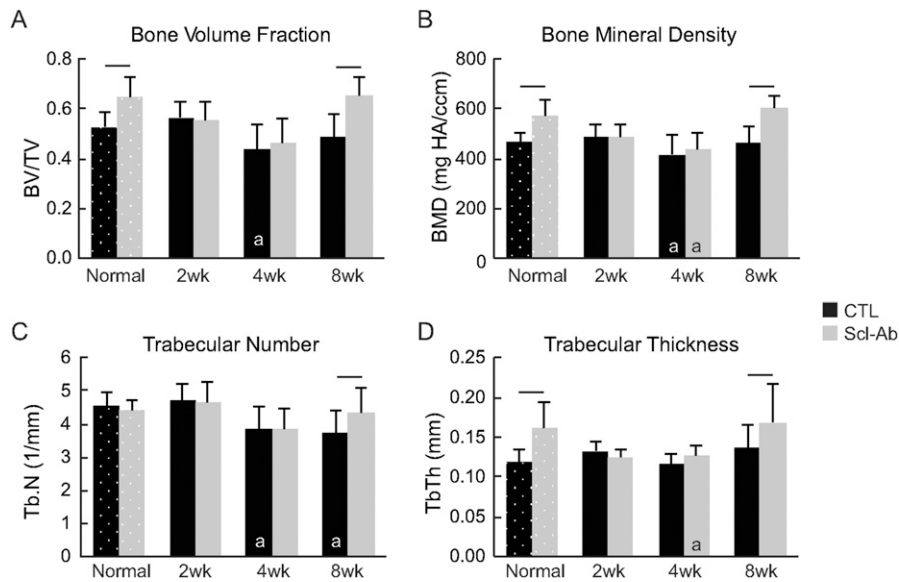


Fig. 1

Treatment with Scl-Ab increased bone volume fraction (BV/TV) (**Fig. 1-A**), bone mineral density (BMD) (**Fig. 1-B**), trabecular number (Tb.N) (**Fig. 1-C**), and/or trabecular thickness (Tb.Th) (**Fig. 1-D**) in the normal (uninjured) and 8-week healing groups. A significant effect of Scl-Ab is indicated by a line over bars ( $p < 0.05$ ; ANOVA followed by Tukey post hoc test compared with CTL within group). A significant difference compared with normal is indicated by an “a” within a bar ( $p < 0.05$ ; ANOVA followed by the Tukey post hoc test compared with normal within a particular treatment group). CTL = control.

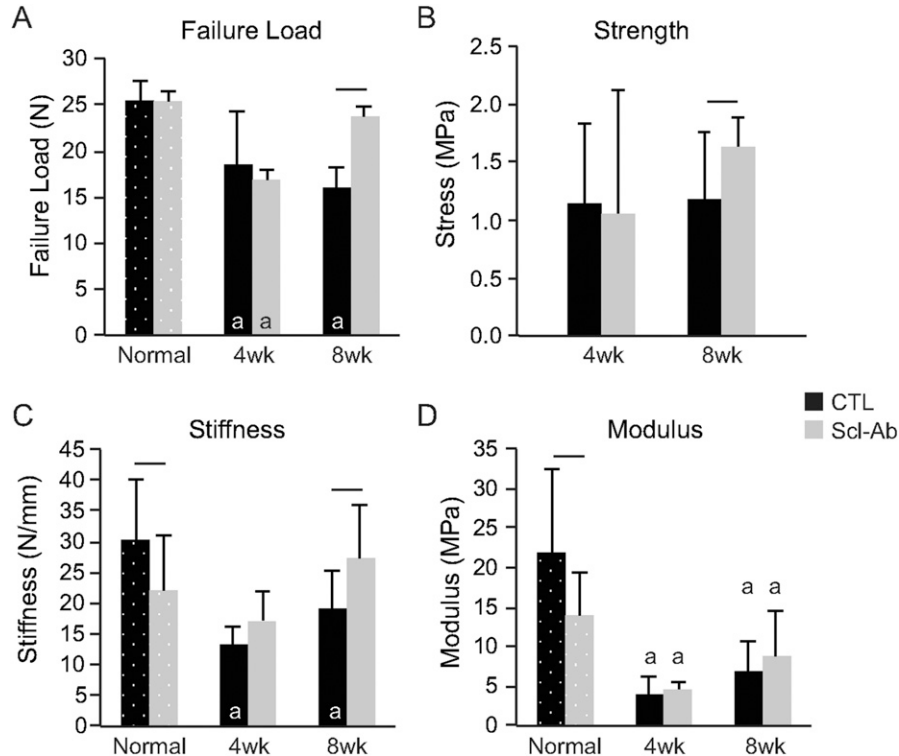


Fig. 2

Treatment with Scl-Ab led to increased attachment-site failure load (**Fig. 2-A**), strength (**Fig. 2-B**), and stiffness (**Fig. 2-C**) after 8 weeks of healing, and stiffness and modulus (**Fig. 2-D**) were decreased in normal (uninjured) attachments. A significant effect of Scl-Ab is indicated by a line over bars ( $p < 0.05$ ; ANOVA followed by Tukey post hoc test compared with CTL within group). A significant difference compared with normal is indicated by an “a” within a bar ( $p < 0.05$ ; ANOVA followed by the Tukey post hoc test compared with normal within a particular treatment group). CTL = control.

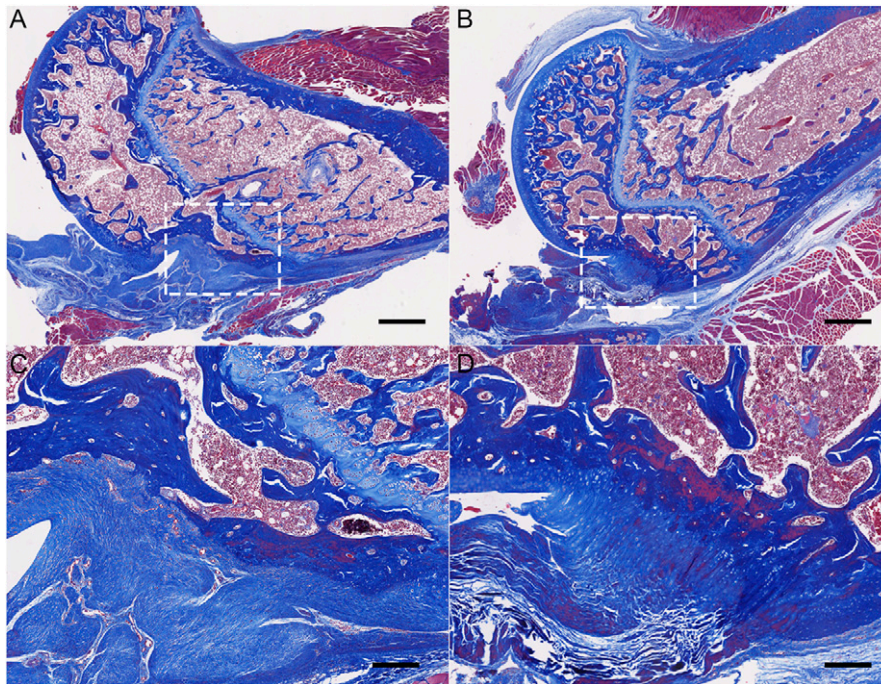


Fig. 3  
Photomicrographs made after 8 weeks of healing show that Scl-Ab treatment (**Figs. 3-B and 3-D**) improved insertion continuity, integrity, and fiber alignment compared with CTL (**Figs. 3-A and 3-C**). The enthesis area is outlined with a white dashed box. Scale bars = 1 mm for Figs. 3-A and 3-B and 250  $\mu$ m for Figs. 3-C and 3-D. Slides were stained with Masson trichrome.

1 to 4 (Table I). A lower score is indicative of improved tendon-to-bone healing, with a score of 9 equivalent to a healthy attachment<sup>24,25</sup>.

### Gene Expression

For gene expression studies (4 per group), humerus-supraspinatus samples were frozen in liquid nitrogen. RNA was isolated separately from the supraspinatus tendon and the portion of the humeral head proximal to the growth

plate near the tendon attachment (RNeasy Kit; Qiagen). RNA was quantified using a NanoDrop 2000 (ThermoFisher Scientific). Quantitative real-time polymerase chain reaction (PCR) was performed using a Biomark HD System (Fluidigm) for tendon and bone RNA on a panel of 25 genes related to bone, tendon, and fibrocartilage (Table II). TaqMan gene expression assays (ThermoFisher Scientific) were used for the analysis. Rpl13a was used as a housekeeping gene, as expression of Rpl13a did not vary more than  $\pm 0.5$  Ct

TABLE III The Modified Tendon-to-Bone Maturity Scores\*

	2 Weeks		4 Weeks		8 Weeks	
	CTL	Scl-Ab	CTL	Scl-Ab	CTL	Scl-Ab
Cellularity	2 (1, 3)	3 (2, 3)	1 (1, 1)	1 (1, 2)	1 (1, 1)	1 (1, 1)
Fibroblasts	2 (1, 2)	2 (2, 2)	1 (1, 1)	1.5 (1.5, 2)	1 (1, 2)	1 (1, 1)
Matrix	4 (1, 4)	2 (2, 3)	3 (2.5, 3)	2.5 (1, 3)	2 (2, 3)	1.5 (1, 2.5)
Cell orientation	3 (1, 3)	2 (2, 3)	2 (2, 3)	1.5 (1, 3)	2 (1, 2)	1 (1, 1)
Collagen orientation	3 (1, 3)	2 (2, 3)	2 (2, 3)	1.5 (1, 3)	2 (1, 2)	1 (1, 1)
Insertion integrity	3 (1, 4)	1.5 (1.5, 2)	2.5 (2.5, 3)	2.5 (1, 2.5)	2.5 (1.5, 3)	1.5 (1, 2.5)
Insertion continuity	3 (1, 4)	2 (2, 3)	3 (3, 3)	3 (1, 3)	2 (1, 3)	1 (1, 2)
Bone resorption	3 (2, 4)	4 (3, 4)	3 (2, 4)	3 (3, 4)	3 (3, 4)	4 (4, 4)
Epiphyseal bone modeling	3 (1, 4)	4 (3, 4)	4 (3, 4)	4 (3, 4)	4 (4, 4)	4 (4, 4)
Overall maturity	24 (14, 29)	22.5 (22, 23.5)	21 (19.5, 25)	20.5 (15.5, 24.5)	21.5 (16.5, 22)	16 (15, 19)

\*The results are shown as the median (minimum, maximum). The modified tendon-to-bone maturity scores improved over time for all groups. Scl-Ab treatment resulted in a more mature attachment at 8 weeks of healing compared with CTL.

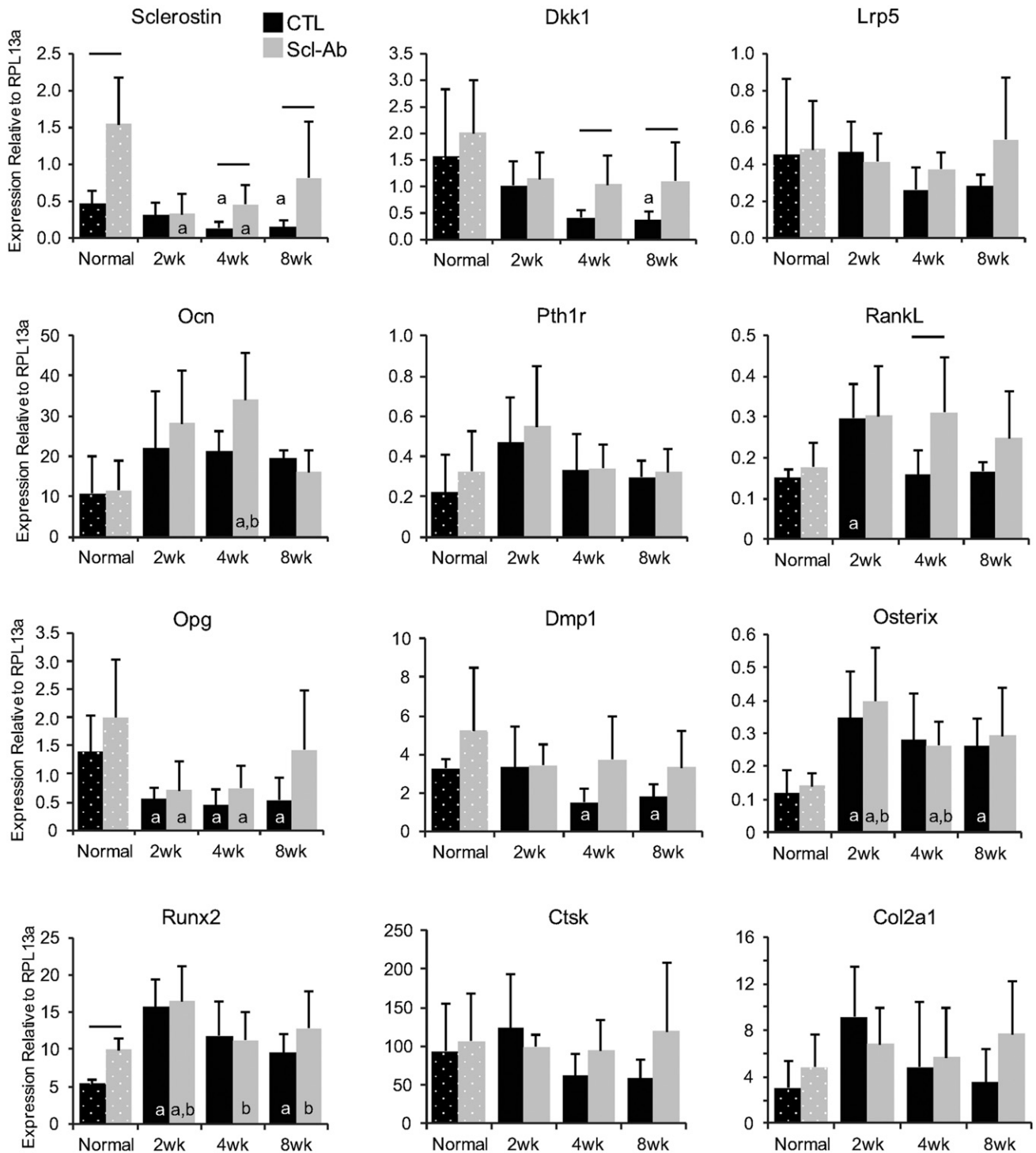
Mineralized Tissue Gene Expression

Fig. 4

Gene expression in mineralized tissue adjacent to the tendon enthesis relative to the housekeeping gene Rpl13a. A significant effect of Scl-Ab is indicated by a line over bars ( $p < 0.05$ ; ANOVA followed by Tukey post hoc test compared with CTL within group). A significant difference compared with normal is indicated by an "a" within a bar ( $p < 0.05$ ; ANOVA followed by Tukey post hoc test compared with normal within a particular treatment group). A significant effect of Scl-Ab compared with normal in the CTL group is indicated by a "b" within a bar ( $p < 0.05$ ; ANOVA followed by the Tukey post hoc test). CTL = control, Pth1r = parathyroid hormone 1 receptor, and Ctsk = cathepsin K.



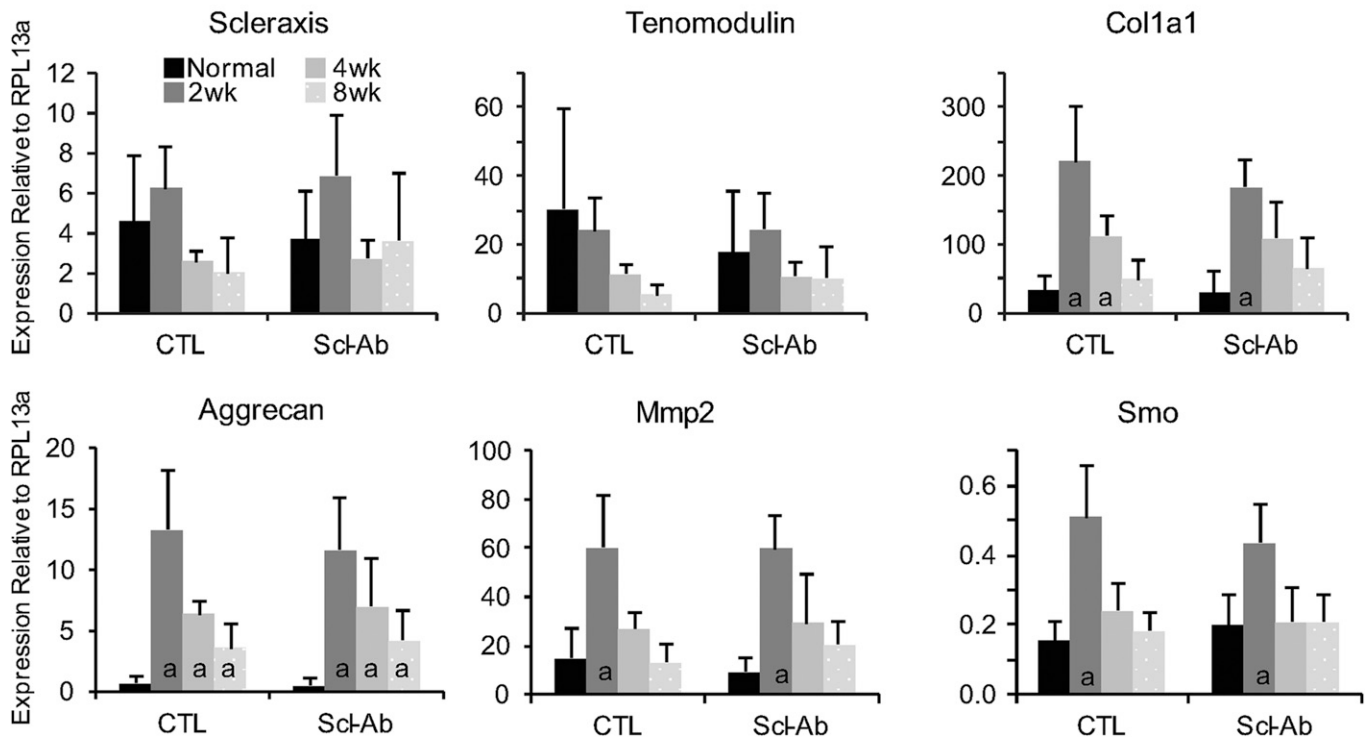
Tendon Gene Expression

Fig. 5

Gene expression in the tendon relative to the housekeeping gene Rpl13a. A significant difference compared with normal is indicated by an "a" within a bar ( $p < 0.05$ ; ANOVA followed by the Tukey post hoc test compared with normal within a particular treatment group).

(cycle threshold value) among groups. Results are presented as relative expression compared with Rpl13a expression ( $2^{-\Delta Ct}$ ).

**Statistical Analysis**

The primary outcome tested in this study was the effect of Scl-Ab treatment. To incorporate the effect of healing duration, a 2-factor analysis of variance (ANOVA), in which the factors analyzed were Scl-Ab treatment and healing time, was performed. When the ANOVA was significant, Tukey post hoc tests were performed to determine specific effects of treatment (CTL or Scl-Ab) and duration of healing (2, 4, or 8 weeks). A secondary outcome tested in this study was the effect of injury and repair. Comparisons between the uninjured control group (the normal group) and the injury-and-repair groups (CTL or Scl-Ab group) were performed using 2-tailed Student t tests. A p value of  $<0.05$  was considered significant for all comparisons. SYSTAT 13 software (Systat Software) was used for all statistical analyses. Error bars in the plotted data represent 1 standard deviation from the mean. Due to the semiquantitative nature of the histological analysis and the low sample size in each group, statistical analysis was not performed on the histological results.

**Results****Bone Morphometry**

There was significant bone loss in the CTL and Scl-Ab groups by 4 weeks of healing, with recovery in the Scl-Ab group by 8 weeks of healing (Fig. 1). Specifically, BV/TV, BMD, and Tb.N in the CTL group and BMD in the Scl-Ab group were significantly decreased compared with the uninjured group at 4 weeks. However, after 8 weeks of healing, in the Scl-Ab treatment

group compared with the CTL group, the BV/TV was increased by 34%, BMD was increased by 30%, Tb.N was increased by 17%, Tb.Th was increased by 24%, and Tb.Sp was decreased by 21% (Fig. 1; see Appendix), reaching levels comparable with those of the uninjured control group. Treatment with Scl-Ab also led to increased BV/TV, BMD, and Tb.Th in the uninjured groups as well. When evaluating the overall effect of Scl-Ab treatment using an ANOVA, Scl-Ab-treated animals had significantly higher BV/TV, BMD, and Tb.Th compared with CTL animals, by 19%, 18%, and 20%, respectively.

**Biomechanical Evaluation**

Eleven of 77 samples were excluded from analysis because they did not fail at the tendon attachment; the excluded samples included 4 operatively treated shoulders from the Scl-Ab group and 4 from the CTL group and 2 non-operatively treated shoulders from the Scl-Ab group and 1 from the CTL group. Injury caused a significant increase in cross-sectional area (mean and standard deviation,  $15.9 \pm 3.9 \text{ mm}^2$  compared with  $6.6 \pm 1.9 \text{ mm}^2$ ). There was a significant decrease in mechanical properties in the CTL and Scl-Ab groups by 4 weeks of healing, with improved mechanical properties in the Scl-Ab group by 8 weeks of healing (Fig. 2; see Appendix). After 8 weeks of healing, comparison of the Scl-Ab treatment and CTL groups demonstrated that failure load was increased by 48%, strength was increased by

38%, and stiffness was increased by 43%. Treatment with Scl-Ab also led to significant decreases in stiffness and modulus in the uninjured groups.

### Histological Analysis

Supraspinatus tendon healing to humeral head bone occurred via a fibrovascular scar, with bone loss evident in the humeral heads of the CTL group (Fig. 3). Based on a blinded analysis of 9 features of the healing tendon-to-bone attachment, the CTL and Scl-Ab healing attachments appeared similar at 2 and 4 weeks of healing (Table III). However, after 8 weeks of healing, the Scl-Ab treatment led to improved insertion continuity, integrity, and fiber alignment compared with the CTL group. The analysis demonstrated a more mature tendon-to-bone attachment and new bone formation in the Scl-Ab group compared with CTL group at 8 weeks (Table III).

### Gene Expression

#### Mineralized Tissues (Bone and Fibrocartilage)

The Scl-Ab treatment had a significant effect on the expression of a number of genes in mineralized tissue near the tendon enthesis, including Sclerostin, Dkk1 (dickkopf-related protein 1), RankL (receptor activator of nuclear factor kappa-B ligand), Dmp1 (dentin matrix acidic phosphoprotein 1), and Runx2 (runt-related transcription factor-2) (Fig. 4). After 8 weeks of healing, expression of Sclerostin and Dkk1 was 3.3 times and 2.5 times greater in the Scl-Ab group compared with the CTL group, respectively. Expression of Lrp5 (low-density lipoprotein receptor-related protein 5) was not affected by treatment or healing time. Osteocalcin (Ocn), a marker of osteoblast activity, was significantly increased following injury, while osteoprotegerin (Opg), a marker of osteoclast inhibition, was significantly decreased after injury in all groups. Expression of RankL and Dmp1 was increased with Scl-Ab treatment (Fig. 4; see Appendix). There was no consistent effect of Scl-Ab treatment on the fibrocartilage-related genes Tgf (transforming growth factor)- $\beta$ 1, Tgf- $\beta$ 3, Mmp (matrix metalloproteinase 2), Col2a1 (collagen type II alpha 1), and Sox9 (Fig. 4; see Appendix). Expression of Smo and Notch1, members of the hedgehog signaling pathway, was not affected by treatment.

#### Tendon Gene Expression

Scl-Ab treatment had no significant effect on tendon gene expression (Fig. 5; see Appendix). Healing time, however, significantly affected all tendon-related genes: Scleraxis, Tenomodulin, Col1a1 (collagen type I alpha 1), Col1a2 (collagen type I alpha 2), and Col3a1 (collagen type III alpha 1). Changes were most apparent at the 2-week healing time point and trended toward normal by the 8-week healing time point. Additionally, expression of aggrecan was 20 times greater in the CTL group and 17 times greater with Scl-Ab treatment after 2 weeks of healing. Similarly, expression of Mmp2 was 4.1 times greater in both the CTL and Scl-Ab treatment groups after 2 weeks of healing.

### Discussion

Rotator cuff injury and repair led to bone loss at the tendon-to-bone interface. A decrease in bone quantity and quality at the healing interface contributes to the high rates of re-tear following surgical repair<sup>3</sup>. Scl-Ab treatment increased bone volume fraction and BMD of the trabecular bone in the humeral head nearest to the healing tendon attachment. Although injury-associated bone loss remained in the treatment group after 8 weeks of healing, rapid recovery toward normal bone was seen by 8 weeks of healing in the treated animals. The improvement in bone morphology at the healing interface had functional consequences, as demonstrated by improved attachment strength. Qualitative histological assessment further confirmed the benefit of Scl-Ab treatment, with a more mature tendon-to-bone interface after 8 weeks of healing in the treated animals compared with control animals.

Delivery of osteoinductive agents such as bone morphogenetic protein-2 to repaired tendon-to-bone attachments has been ineffective in improving healing<sup>24,26</sup>. However, bisphosphonates have previously shown success in improving tendon-to-bone healing by reducing bone resorption<sup>16,27</sup>. In a canine model of flexor tendon-to-bone healing, tendon injury caused BMD near the tendon-to-bone interface to decrease by 29% compared with normal after 21 days<sup>16</sup>. An oral dose of alendronate was effective in preventing bone resorption, leading to only a 6% decrease in BMD compared with normal. The prevention of bone loss resulted in a significant improvement in the failure load of the repair after 21 days of healing. In a separate study, subcutaneous injections of zoledronic acid to ovariectomized rats resulted in a 23% increase in BMD of the humeral head near the supraspinatus tendon insertion compared with the control<sup>27</sup>. The increased BMD was associated with a 24% increase in failure load at the interface following treatment. In the current study, after 8 weeks of healing, Scl-Ab treatment caused a 30% increase in BMD and a 48% increase in failure load compared with the control, consistent with the prior bisphosphonate treatment approaches.

The Scl-Ab used in the current study has been previously shown to neutralize sclerostin by preventing sclerostin binding to the Lrp5 receptor<sup>28-30</sup>. To determine whether improvements in bone morphology during tendon-to-bone healing were achieved through this mechanism, we measured expression of Wnt signaling-related genes in the mineralized tissues at the healing attachment. Scl-Ab treatment increased expression of the Wnt-target genes sclerostin and Dkk1 relative to control during tendon-to-bone-healing, in contrast to decreases observed in controls relative to normal, uninjured attachments. The changes observed in the Scl-Ab group indicate a compensatory cellular response to chronic use of Scl-Ab treatment, as described by Taylor et al.<sup>31</sup>. Further analysis of bone-related gene expression showed a reduction of osteoclast inhibition (as demonstrated by an increase in Opg relative to RankL) and an increase in osteoblast activity (as demonstrated by increased osteocalcin) with Scl-Ab, consistent with the observed improvements in bone morphology. Genes related to osteoprogenitors (Osterix and Runx2) were significantly increased with

injury compared with normal, uninjured groups. These genes, however, were not affected by treatment in healing bone, although Runx2 was increased by Scl-Ab in normal, uninjured bone. Increased expression of these factors, which are also associated with differentiation of mesenchymal cells into osteoblasts<sup>32,33</sup>, suggests the possible induction of bone formation via progenitors as well as mature osteoblasts.

The strength of the tendon attachment is in large part dictated by the quality of the mineralized tissue at the interface<sup>34,35</sup>. The healthy tendon-to-bone attachment has a gradient of mineral content across the fibrocartilaginous insertion and into the trabecular bone<sup>36</sup>. The increase in mechanical strength at the attachment because of Scl-Ab treatment is likely the result of improved mineralization in not only the trabecular bone compartment (as measured by microCT) but also the fibrocartilage at the healing interface. Expression of aggrecan, an extracellular matrix marker of cartilage and fibrocartilage, was significantly higher with Scl-Ab treatment after 8 weeks of healing. Furthermore, blinded evaluation of histological sections showed improvements in tendon-to-bone attachment maturity, including insertion integrity, after 4 and 8 weeks of healing with Scl-Ab treatment compared with controls.

Scl-Ab was administered by subcutaneous injection; therefore, all tissues were exposed to the antibody, including the tendon adjacent to the healing interface. To evaluate possible effects of Scl-Ab on nonmineralized tissues, gene expression was examined in the supraspinatus tendon adjacent to the healing interface. Scl-Ab treatment did not have a significant effect on expression of genes in tendon tissue, alleviating the concern of possible effects of treatment on off-target tissue. However, Scl-Ab treatment did lead to a decrease in modulus and stiffness in healthy tendon-to-bone attachments. This result is consistent with a previous finding that bisphosphonate treatment during tendon-to-bone healing can cause a decrease in stiffness<sup>16</sup>. Due to the high mechanical safety factor of tendons and ligaments for typical physiologic activities<sup>37</sup>, the relatively small decreases in stiffness and modulus may not predispose healthy tendons to injury. However, possible consequences of the reduced stiffness and modulus at uninjured attachments should be further considered.

There were several limitations to the current study. The animal model consisted of an acute injury and repair. In contrast, most rotator cuff tears in the clinical population occur after chronic tendon degeneration. Bone loss in these cases may therefore be more severe than in the current animal study. It is unclear whether Scl-Ab treatment would be effective in the chronic injury scenario, although studies have shown efficacy of the treatment approach in the context of osteoporosis<sup>20-22</sup>. Additional animal and clinical studies are necessary to test this premise. A second limitation of this study was the use of subcutaneous (i.e., systemic) high-dose injections of Scl-Ab. This dosing regimen (25 mg/kg every 2 weeks) has been reported in

proof-of-concept studies across various animal models<sup>38-40</sup>, although future studies would be required to determine the dose-response to Scl-Ab for tendon-to-bone healing and potential application of Scl-Ab via local delivery. Finally, an additional control group consisting of vehicle injection would have strengthened the study design. In the current study, treatment was compared with the equivalent of “standard of care,” i.e., repair only without additional biologic treatment.

In conclusion, bone loss was observed at the healing tendon-to-bone interface, contributing to poor outcomes. Treatment with Scl-Ab improved healing by increasing attachment-site BMD, leading to improved biomechanical properties. Considering recent evidence that Scl-Ab (i.e., romosozumab, for human use) is safe and effective for treating osteoporosis in humans<sup>20,41</sup>, the results from the current study support the use of the treatment in combination with repair of acute rotator cuff tears. Treatment is expected to enhance tendon-to-bone repair, by improving bone morphology and tendon insertion maturity, leading to improved tendon attachment strength.

## Appendix

**eA** Figures demonstrating the effect of treatment with Scl-Ab and 8 weeks of healing on trabecular spacing and resilience, gene expression in mineralized tissue adjacent to the tendon enthesis, and gene expression in the tendon are available with the online version of this article as a data supplement at [jbjs.org \(http://links.lww.com/JBJS/D273\)](http://links.lww.com/JBJS/D273). ■

Shivam A. Shah, PhD<sup>1</sup>  
Ioannis Korpakakis, MD<sup>1</sup>  
Necat Havlioglu, MD<sup>2</sup>  
Michael S. Ominsky, PhD<sup>3</sup>  
Leesa M. Galatz, MD<sup>4</sup>  
Stavros Thomopoulos, PhD<sup>5</sup>

<sup>1</sup>Department of Orthopaedic Surgery, Washington University in St. Louis, St. Louis, Missouri

<sup>2</sup>Department of Pathology, John Cochran VA Medical Center, St. Louis, Missouri

<sup>3</sup>Metabolic Disorders Research, Amgen, Inc., Thousand Oaks, California

<sup>4</sup>Department of Orthopedic Surgery, Icahn School of Medicine, Mount Sinai Health System, New York, NY

<sup>5</sup>Department of Orthopedic Surgery, Department of Biomedical Engineering, Columbia University, New York, NY

E-mail address for S. Thomopoulos: [sat2@columbia.edu](mailto:sat2@columbia.edu)

## References

1. Keener JD, Galatz LM, Teefey SA, Middleton WD, Steger-May K, Stobbs-Cucchi G, Patton R, Yamaguchi K. A prospective evaluation of survivorship of asymptomatic degenerative rotator cuff tears. *J Bone Joint Surg Am.* 2015 Jan 21;97(2):89-98.

2. Colvin AC, Egorova N, Harrison AK, Moskowitz A, Flatow EL. National trends in rotator cuff repair. *J Bone Joint Surg Am.* 2012 Feb 01;94(3):227-33. Epub 2012 Feb 3.

3. Galatz LM, Ball CM, Teefey SA, Middleton WD, Yamaguchi K. The outcome and repair integrity of completely arthroscopically repaired large and massive rotator cuff tears. *J Bone Joint Surg Am*. 2004 Feb;86(2):219-24.
4. Thomopoulos S, Birman V, Genin GM. Structural interfaces and attachments in biology. New York: Springer; 2013.
5. Galatz LM, Charlton N, Das R, Kim HM, Havlioglu N, Thomopoulos S. Complete removal of load is detrimental to rotator cuff healing. *J Shoulder Elbow Surg*. 2009 Sep-Oct;18(5):669-75. Epub 2009 May 8.
6. Galatz LM, Rothermich SY, Zaegel M, Silva MJ, Havlioglu N, Thomopoulos S. Delayed repair of tendon to bone injuries leads to decreased biomechanical properties and bone loss. *J Orthop Res*. 2005 Nov;23(6):1441-7. Epub 2005 Aug 1.
7. Gimbel JA, Van Kleunen JP, Lake SP, Williams GR, Soslowsky LJ. The role of repair tension on tendon to bone healing in an animal model of chronic rotator cuff tears. *J Biomech*. 2007;40(3):561-8. Epub 2006 Apr 4.
8. Thomopoulos S, Kim HM, Rothermich SY, Biederstadt C, Das R, Galatz LM. Decreased muscle loading delays maturation of the tendon enthesis during post-natal development. *J Orthop Res*. 2007 Sep;25(9):1154-63. Epub 2007 May 18.
9. Thomopoulos S, Zampiakos E, Das R, Silva MJ, Gelberman RH. The effect of muscle loading on flexor tendon-to-bone healing in a canine model. *J Orthop Res*. 2008 Dec;26(12):1611-7.
10. Leppälä J, Kannus P, Natri A, Pasanen M, Sievänen H, Vuori I, Järvinen M. Effect of anterior cruciate ligament injury of the knee on bone mineral density of the spine and affected lower extremity: a prospective one-year follow-up study. *Calcif Tissue Int*. 1999 Apr;64(4):357-63.
11. Alfredson H, Nordström P, Lorentzon R. Prolonged progressive calcaneal bone loss despite early weightbearing rehabilitation in patients surgically treated for Achilles tendinosis. *Calcif Tissue Int*. 1998 Feb;62(2):166-71.
12. Silva MJ, Ritty TM, Ditsios K, Burns ME, Boyer MI, Gelberman RH. Tendon injury response: assessment of biomechanical properties, tissue morphology and viability following flexor digitorum profundus tendon transection. *J Orthop Res*. 2004 Sep;22(5):990-7.
13. Killian ML, Cavinatto L, Shah SA, Sato EJ, Ward SR, Havlioglu N, Galatz LM, Thomopoulos S. The effects of chronic unloading and gap formation on tendon-to-bone healing in a rat model of massive rotator cuff tears. *J Orthop Res*. 2014 Mar;32(3):439-47. Epub 2013 Nov 14.
14. Killian ML, Cavinatto LM, Ward SR, Havlioglu N, Thomopoulos S, Galatz LM. Chronic degeneration leads to poor healing of repaired massive rotator cuff tears in rats. *Am J Sports Med*. 2015 Oct;43(10):2401-10. Epub 2015 Aug 21.
15. Ditsios K, Boyer MI, Kusano N, Gelberman RH, Silva MJ. Bone loss following tendon laceration, repair and passive mobilization. *J Orthop Res*. 2003 Nov;21(6):990-6.
16. Thomopoulos S, Matsuzaki H, Zaegel M, Gelberman RH, Silva MJ. Alendronate prevents bone loss and improves tendon-to-bone repair strength in a canine model. *J Orthop Res*. 2007 Apr;25(4):473-9.
17. Kennel KA, Drake MT. Adverse effects of bisphosphonates: implications for osteoporosis management. *Mayo Clin Proc*. 2009 Jul;84(7):632-7, quiz :638.
18. Bone HG, Hosking D, Devogelaer JP, Tucci JR, Emkey RD, Tonino RP, Rodriguez-Portales JA, Downs RW, Gupta J, Santora AC, Liberman UA; Alendronate Phase III Osteoporosis Treatment Study Group. Ten years' experience with alendronate for osteoporosis in postmenopausal women. *N Engl J Med*. 2004 Mar 18;350(12):1189-99.
19. Black DM, Schwartz AV, Ensrud KE, Cauley JA, Levis S, Quandt SA, Satterfield S, Wallace RB, Bauer DC, Palermo L, Wehren LE, Lombardi A, Santora AC, Cummings SR; FLEX Research Group. Effects of continuing or stopping alendronate after 5 years of treatment: the Fracture Intervention Trial Long-term Extension (FLEX): a randomized trial. *JAMA*. 2006 Dec 27;296(24):2927-38.
20. McClung MR, Grauer A, Boonen S, Bolognese MA, Brown JP, Diez-Perez A, Langdahl BL, Reginster JY, Zanchetta JR, Wasserman SM, Katz L, Maddox J, Yang YC, Libanati C, Bone HG. Romosozumab in postmenopausal women with low bone mineral density. *N Engl J Med*. 2014 Jan 30;370(5):412-20. Epub 2014 Jan 1.
21. Padhi D, Jang G, Stouch B, Fang L, Posvar E. Single-dose, placebo-controlled, randomized study of AMG 785, a sclerostin monoclonal antibody. *J Bone Miner Res*. 2011 Jan;26(1):19-26.
22. Li X, Ominsky MS, Warmington KS, Morony S, Gong J, Cao J, Gao Y, Shalhoub V, Tipton B, Haldankar R, Chen Q, Winters A, Boone T, Geng Z, Niu QT, Ke HZ, Kostenuik PJ, Simonet WS, Lacey DL, Paszty C. Sclerostin antibody treatment increases bone formation, bone mass, and bone strength in a rat model of postmenopausal osteoporosis. *J Bone Miner Res*. 2009 Apr;24(4):578-88.
23. Manning CN, Kim HM, Sakiyama-Elbert S, Galatz LM, Havlioglu N, Thomopoulos S. Sustained delivery of transforming growth factor three enhances tendon-to-bone healing in a rat model. *J Orthop Res*. 2011 Jul;29(7):1099-105. Epub 2011 Jan 18.
24. Lipner J, Shen H, Cavinatto L, Liu W, Havlioglu N, Xia Y, Galatz LM, Thomopoulos S. In vivo evaluation of adipose-derived stromal cells delivered with a nanofiber scaffold for tendon-to-bone repair. *Tissue Eng Part A*. 2015 Nov;21(21-22):2766-74. Epub 2015 Oct 20.
25. Ide J, Kikukawa K, Hirose J, Iyama K, Sakamoto H, Fujimoto T, Mizuta H. The effect of a local application of fibroblast growth factor-2 on tendon-to-bone remodeling in rats with acute injury and repair of the supraspinatus tendon. *J Shoulder Elbow Surg*. 2009 May-Jun;18(3):391-8.
26. Thomopoulos S, Kim HM, Silva MJ, Ntouvali E, Manning CN, Potter R, Seeherman H, Gelberman RH. Effect of bone morphogenetic protein 2 on tendon-to-bone healing in a canine flexor tendon model. *J Orthop Res*. 2012 Nov;30(11):1702-9. Epub 2012 May 22.
27. Cadet ER, Vorys GC, Rahman R, Park SH, Gardner TR, Lee FY, Levine WN, Bigliani LU, Ahmad CS. Improving bone density at the rotator cuff footprint increases supraspinatus tendon failure stress in a rat model. *J Orthop Res*. 2010 Mar;28(3):308-14.
28. Sinder BP, Salemi JD, Ominsky MS, Caird MS, Marini JC, Kozloff KM. Rapidly growing Brl/+ mouse model of osteogenesis imperfecta improves bone mass and strength with sclerostin antibody treatment. *Bone*. 2015 Feb;71:115-23. Epub 2014 Oct 23.
29. Li X, Zhang Y, Kang H, Liu W, Liu P, Zhang J, et al. Sclerostin binds to LRP5/6 and antagonizes canonical Wnt signaling. *J Biol Chem*. 2005;280(20):19883-7.
30. Veverka V, Henry AJ, Slocombe PM, Ventom A, Mulloy B, Muskett FW, Muzylak M, Greenslade K, Moore A, Zhang L, Gong J, Qian X, Paszty C, Taylor RJ, Robinson MK, Carr MD. Characterization of the structural features and interactions of sclerostin: molecular insight into a key regulator of Wnt-mediated bone formation. *J Biol Chem*. 2009 Apr 17;284(16):10890-900. Epub 2009 Feb 10.
31. Taylor S, Ominsky MS, Hu R, Pacheco E, He YD, Brown DL, Aguirre JI, Wronski TJ, Buntich S, Afshari CA, Pyrah I, Nioi P, Boyce RW. Time-dependent cellular and transcriptional changes in the osteoblast lineage associated with sclerostin antibody treatment in ovariectomized rats. *Bone*. 2016 Mar;84:148-59. Epub 2015 Dec 22.
32. Komori T. Regulation of osteoblast differentiation by transcription factors. *J Cell Biochem*. 2006 Dec 01;99(5):1233-9.
33. Nakashima K, Zhou X, Kunkel G, Zhang Z, Deng JM, Behringer RR, de Crombrughe B. The novel zinc finger-containing transcription factor osterix is required for osteoblast differentiation and bone formation. *Cell*. 2002 Jan 11;108(1):17-29.
34. Genin GM, Kent A, Birman V, Wopenka B, Pasteris JD, Marquez PJ, Thomopoulos S. Functional grading of mineral and collagen in the attachment of tendon to bone. *Biophys J*. 2009 Aug 19;97(4):976-85. Epub 2009 Aug 19.
35. Schwartz AG, Lipner JH, Pasteris JD, Genin GM, Thomopoulos S. Muscle loading is necessary for the formation of a functional tendon enthesis. *Bone*. 2013 Jul;55(1):44-51. Epub 2013 Mar 29.
36. Schwartz AG, Pasteris JD, Genin GM, Daulton TL, Thomopoulos S. Mineral distributions at the developing tendon enthesis. *PLoS One*. 2012;7(11):e48630. Epub 2012 Nov 9.
37. West JR, Juncosa N, Galloway MT, Boivin GP, Butler DL. Characterization of in vivo Achilles tendon forces in rabbits during treadmill locomotion at varying speeds and inclinations. *J Biomech*. 2004 Nov;37(11):1647-53.
38. Ominsky MS, Vlasseros F, Jolette J, Smith SY, Stouch B, Doelligast G, Gong J, Gao Y, Cao J, Graham K, Tipton B, Cai J, Deshpande R, Zhou L, Hale MD, Lightwood DJ, Henry AJ, Popplewell AG, Moore AR, Robinson MK, Lacey DL, Simonet WS, Paszty C. Two doses of sclerostin antibody in cynomolgus monkeys increases bone formation, bone mineral density, and bone strength. *J Bone Miner Res*. 2010 May;25(5):948-59.
39. Tian X, Jee WS, Li X, Paszty C, Ke HZ. Sclerostin antibody increases bone mass by stimulating bone formation and inhibiting bone resorption in a hindlimb-immobilization rat model. *Bone*. 2011 Feb;48(2):197-201. Epub 2010 Sep 17.
40. Li X, Warmington KS, Niu QT, Asuncion FJ, Barrero M, Grisanti M, Dwyer D, Stouch B, Thway TM, Stolina M, Ominsky MS, Kostenuik PJ, Simonet WS, Paszty C, Ke HZ. Inhibition of sclerostin by monoclonal antibody increases bone formation, bone mass, and bone strength in aged male rats. *J Bone Miner Res*. 2010 Dec;25(12):2647-56. Epub 2010 Jul 16.
41. Chouinard L, Felix M, Mellal N, Varela A, Mann P, Jolette J, Samadifam R, Smith SY, Locher K, Buntich S, Ominsky MS, Pyrah I, Boyce RW. Carcinogenicity risk assessment of romosozumab: a review of scientific weight-of-evidence and findings in a rat lifetime pharmacology study. *Regul Toxicol Pharmacol*. 2016 Nov;81:212-22. Epub 2016 Aug 26.